Experimental investigation of difference in indoor environment using impinging jet ventilation and displacement ventilation systems

Haruna Yamasawa , Tomohiro Kobayashi , Toshio Yamanaka , Narae Choi & Mako Matsuzaki

Published online: 27 Jan 2021.

Submit your article to this journal ⍑

View related articles ⍑

View Crossmark data ⍑

Taylor & Francis
Taylor & Francis Group

Check for updates

Experimental investigation of difference in indoor environment using impinging jet ventilation and displacement ventilation systems

Haruna Yamasawa [ID], Tomohiro Kobayashi, Toshio Yamanaka [ID], Narae Choi and Mako Matsuzaki*

Department of Architectural Engineering, Osaka University, Suita, Osaka, Japan

ABSTRACT

The impinging jet ventilation (IJV) system has been proposed as a new air distribution strategy and is expected to overcome the disadvantages of mixing ventilation (MV) system, which is the most widely used system, and displacement ventilation (DV), which provides better air quality than MV. The aim of this study is to accumulate the fundamental feature of IJV and to propose a simple method to predict the indoor environment with IJV. Full-scale experiments were conducted in a climate chamber, in order to investigate the features of IJV. Different ventilation systems and supply air conditions were investigated along with indoor thermal environments, and ventilation effectiveness. For IJV, the indoor environment was similar to that of DV with small supply momentum, and was similar to that of MV with large supply momentum. The specific Archimedes number, which can be calculated by design conditions, was defined to express the balance between the supply momentum and buoyancy force. The correlation between the Archimedes number and indices for thermal environment and ventilation effectiveness are finally shown as prediction method.

Abbreviations: CFD: computational fluid dynamics; CRE: contaminant removal effectiveness; DV: displacement ventilation; FL: floor level; IJV: impinging jet ventilation; MV: mixing ventilation; RNG k-ε: renormalised group k-ε; SST k-ω: sheer-stress transport k-ω

1. Introduction

The mixing ventilation (MV) system has been the most popular and widely used air conditioning system for decades. However, in MV, the entire air in the room is mixed and diluted with supplied air to maintain the air quality; therefore, the contaminated air spreads through the room, even to areas that were not originally contaminated (Boyle, 1899). Accordingly, the displacement ventilation (DV) system (Mundt, 1995; Suzuki et al., 2007; Xu et al., 2001; Yuan et al., 1998) was introduced to improve the ventilation effectiveness. In DV, the cooled air is supplied to the lower level of the room with low momentum. The supplied cooled air spreads through the lower level of the room until it reaches the heat sources. It rises upward within the thermal plume generated from the heat sources, along with contaminated air. In a room with DV, vertical

Nomenclature

Ar_{room}	Archimedes number ($= g\beta H_c(T_e - T_s)/v_s^2$) (-)	T_{Ak}	Average temperature around ankle (0–0.3 m) (°C)
C_h	Horizontal-average CO_2 concentration at the height of h (ppm)	T_e	Temperature of exhaust air (°C)
C_e	CO_2 concentration of exhaust air (ppm)	T_s	Temperature of supply air (°C)
C_s	CO_2 concentration of supply air (ppm)	ΔT(°C)	Temperature difference between exhaust and supply air ($T_e - T_s$)
C_h^*	Dimensionless CO_2 concentration at each height (-)	T_{Ak}^* (-)	Dimensionless temperature around ankle ($= \{T_{0.1} - T_s\}/(T_e - T_s)$)
C_n	Dimensionless CO_2 concentration within occupied zone ($= \{\langle C_{1.8}\rangle - C_s\}/(C_e - C_s)$) (-)	$T_{OZ-h_{oz}}^*$(-)	Dimensionless temperature within occupied zone
g	Gravity acceleration ($= 9.8$) (m/s²)	$T_{VD-h_{oz}}^*$(-)	Dimensionless vertical temperature difference between head and ankle
h	Height (m)	v_s	Velocity of supply air (m/s)
H_c	Height of room ($= 2.7$) (m)	β	Volume expansion coefficient ($= 0.00345$) (1/K)
h_{oz}	Height of occupied zone ($h_{oz} = 1.1$ (m) when sitting and $h_{oz} = 1.7$ (m) when standing) (m)	ε^c	Contaminant removal effectiveness (CRE) ($= (C_e - C_s)/\{\langle C_{room}\rangle - C_s\}$) (-)
T_h	Horizontal-average temperature at the height of h (°C)		

stratifications of temperature and contaminants are formed, i.e. the lower level of the room is kept cooler and cleaner. In a stratified ventilation system, such as DV, it is the occupied zone that must be kept comfortable. Thus, compared to MV, which is based on the idea of dilution, DV can keep the occupied zone clean.

The pros and cons of DV were actively researched in the late 1980s (Mathisen, 1989; Melikov & Nielsen, 1989; Sandberg & Blomqvist, 1989; Seppanen et al., 1989; Svensson, 1989), and Nielsen summarised the information about DV to a book at 1993 (Nielsen, 1993). Following the above-described works, further advanced research was conducted about personal exposure (Brohus & Nielsen, 1996), the ventilation effectiveness in breathing zone (Xing et al., 2001), enhancement of air transport (Sun et al., 2012), and key index in DV (Fatemi et al., 2013). In addition, the computational analysis was conducted to investigate these parameters further (Lin et al., 2007; Park & Holland, 2001; Yuan, Chen, Glicksman, Hu, et al., 1999). Moreover, some calculation models were developed to predict the indoor environment of a room with DV (Habchi et al., 2015; Li et al., 1992; Wu et al., 2013; Yamanaka et al., 2007; Yuan, Chen, & Glicksman, 1999). However, DV also has shortcomings. Since air is supplied with low velocity in this system, there is a possibility that the supplied air rises upwards before it reaches the inner area of the room. For the same reason, DV cannot be applied for space heating. Additionally, since DV supplies the cooled air directly to the occupied zone, there is an overcooling risk around the ankle level.

To overcome the disadvantages of MV and DV, the impinging jet technique (Assoum et al., 2020; Rajaratnam, 1976) was applied to the ventilation system as a new air distribution strategy (Cao et al., 2010; Kobayashi et al., 2019; Ye et al., 2016, 2019). In impinging jet ventilation (IJV) system, which also is a stratified ventilation system, the cooled air is supplied downward via a jet to a room, and once it strikes (impinges) the floor, the supplied air spreads through the room horizontally in a thin layer. With using IJV, it is expected that one can decrease the overcooling risk around floor, which is the disadvantage of DV, due to the higher momentum while keeping high ventilation effectiveness like DV. In order to understand the ventilation characteristic of IJV, several different air distribution systems were compared (Ameen et al., 2019; Awbi &

Karimipanah, 2002; Karimipanah et al., 2000; Karimipanah & Awbi, 2002). To understand more about this newly proposed air distribution strategy, parametric studies are required, and computational fluid dynamics (CFD) is an effective way for it, because it is possible to set the parameters easier than experiments. Several CFD analysis was conducted for understanding key parameters in IJV (Chen et al., 2012; Chen, Moshfegh, & Cehlin, 2013; Chen Moshfegh, & Mathias, 2013), verifying analysis method (Kobayashi et al., 2017), and investigating optimal design for IJV (Ye et al., 2020). Additionally, some investigation showed the advantages of IJV under heating mode compared to MV (Ye et al., 2016, 2017, 2018).

Although some studies have been done to understand the features of IJV as reviewed above, few studies have been done to propose a simplified prediction method of the indoor environment for the room with IJV, that is available in the design phase. For instance, Nielsen proposed the idea of 'family tree' for interconnecting different type of air distribution systems for cooling with using three-dimensional chart (Nielsen, 2001). He claimed that by collecting and organising the data by Archimedes number, it is possible to clarify the feature of flow pattern. This seems to be logically rational concept which is also valid for IJV system. To date, however, the data required for practical prediction of the indoor environment for IJV has not been sufficiently organised. In a room with IJV, the distribution of temperature and contaminant varies between that of DV and MV depending on several design conditions. It has not been well understood to what extent some important parameters like Archimedes number should be adjusted to achieve intended stratification in IJV system. In this context, further knowledge must be accumulated.

Therefore, in this paper, there are two purposes: One is to understand how the indoor temperature and contaminant concentration distribution changes depending on the supply conditions, i.e. depending on the specific Archimedes number, which has not yet been sufficiently clarified. The other is to propose a simple prediction method of some important indices regarding thermal environment and ventilation effectiveness for IJV, which is available in the design phase to determine supply condition.

The experiment is conducted in a climate chamber with heating elements distributed inside. For both IJV and DV, supply air conditions are the adjusted parameters. To understand the effect of the correlation between supply airflow momentum and buoyancy, the indoor temperature and contaminant distribution are measured. Some of the results are expressed in normalised form such as dimensionless temperature or ventilation effectiveness as important indices. The specific Archimedes number is used to predict these indices and the correlations are arranged, which seem to be of use for simplified estimation in the preliminary/working design phase, and have never been organised for IJV system to date. Consequently, the empirical equations are to be provided in the present paper.

2. Experimental methods

2.1. Experimental set-up

Experiments were conducted from November 2019 to February 2020 at a climate chamber of which floor area is 27.25 m^2. The inner size of the chamber was 5,450 mm (width) $\times$ 5,000 mm (depth) $\times$ 2,770 mm (height) and was located in the main laboratory of Osaka University, Japan. The floor plan and cross-section of the climate chamber are shown in Figure 1.

At the middle of each north and south wall, a round duct with a diameter of 150 mm was installed as IJV supply terminal. The bottom end of each duct was set at a distance of 600 mm above the floor. The IJV terminals were insulated by polyethylene foam sheets. The supply airflow rate was adjusted using a volume damper and an orifice flow metre (Iris Damper, Continental Fan). The exhaust opening was located approximately at the centre of the ceiling. Here, the exhausted air from the room never returns to the air handling unit, and all-fresh air conditioning system was operated. As heating elements, twenty black lamps (incandescent bulbs
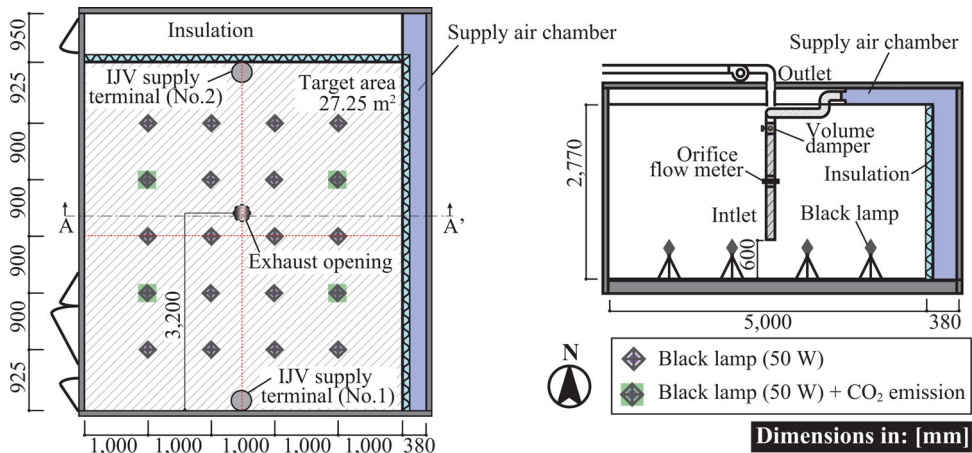
Figure 1. Experimental set-ups (Left: Floor plan, Right: A-A' Cross-Section).
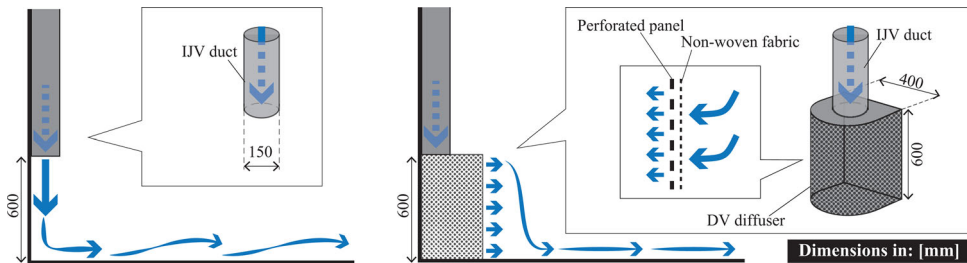

Figure 2. Supply terminals and the schematic of supplied air flow from each terminal (Left: IJV, Right: DV).

covered with dark purple glass), whose heat generation rate was 50 W each, were distributed in the chamber. Since its luminous efficiency is quite low, most of the electrical power is used for generating heat, and the portion of convective heat from black lamp is approximately 82%.

The heating elements were originally prepared for simulating the heat generation from seated human and other apparatus. In this paper, for simplicity, all of the heating elements were assumed to be simulated by cylinder of the same shape. Moreover, to facilitate the experiment, black lamp was adopted instead of cylinder. Skistad (Skistad, 1994) provided the method to locate point heat source to replace the cylinder with heat generation rate of 50 W. He provided the equation for calculating the installation height of the point heat source that generates the same convection current as that of the specific cylinder heat source. In order to simulate the convection current from the cylinder with a diameter of 400 mm and a height of 1,100 mm, which simulates a seated human, the point heat source should be located at the height of 511 mm. Therefore, the black lamps were located at the height of 500 mm as point heat source. Four of the black lamps were chosen for simulating the emission of contaminant generated from a human. A vinyl tube, which provided CO_2 gas as the contaminant from a human, was fixed over each of the four black lamps. To decrease the initial velocity of CO_2 emission, the emission-end of the tubes was inserted into sponges.

To understand the effect of supply momentum and supply temperature on indoor environment in IJV system and its difference from DV system, both IJV and DV are tested and the results of temperature/CO_2 concentration are compared between these two systems in this paper. The supply terminal of each ventilation system is shown in Figure 2. When conducting an experiment for the cases of DV, a DV terminal was attached to the bottom end of IJV terminal as shown in Figure 1. The height of the DV terminal was 600 mm and the net opening area of supply surface,
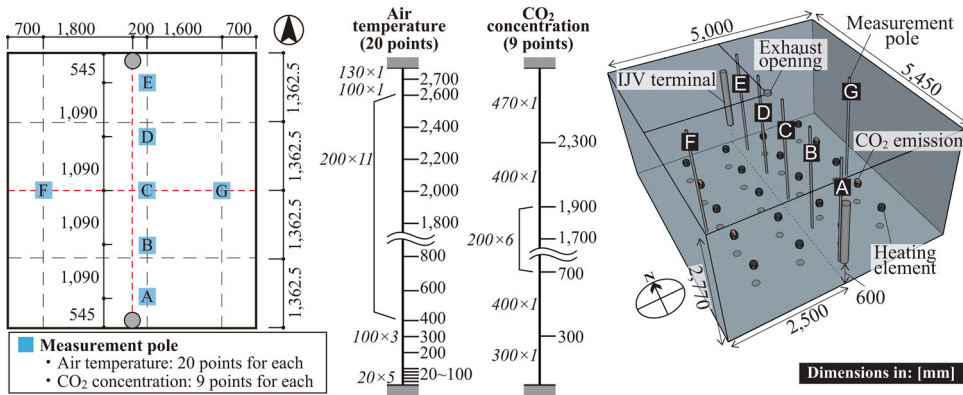
Figure 3. Measurement points (Left: Horizontal distribution of measurement poles, Middle: Vertical distribution of measurement points, Right: Overview of climate chamber).

which was made of a curved perforated panel with a porosity of 40.3%, was 0.188 m^2. Inside the supply plane, non-woven fabric was installed for uniform velocity distribution.

The vertical distributions of the temperature and CO_2 concentration were measured along seven poles arranged from setting points A to G shown in Figure 3. The setting point of the vertical poles along the north-south line (pole A to E) was aligned with a distance of 200 mm from the central line so as not to disturb the development of the jet along the floor on the central cross-section. As for the number of measurement point, for each vertical pole, the air temperature was measured at 20 points by using T-type thermocouples, i.e. 20 points × 7 poles = 140 measurement points in total for air temperature. The T-type thermocouples used in this paper are ASTM E230 Standard class, whose tolerance is ± 1.0 °C or ± 0.75%. Regarding CO_2 concentration, 9 portable CO_2 concentration recorders were provided for each pole, which means 63 measurement points for CO_2 concentration of the room air in total. The height of measurement points is illustrated in Figure 3, and an overview of the climate chamber is also shown in Figure 3. Additionally, CO_2 concentration was also measured at two more measuring points, i.e. at the supply air chamber and exhaust duct. The CO_2 recorders with NDIR sensor were used. In order to minimise the error of measured concentration results, calibration for all sixty-five CO_2 recorders took place. By using span gases with four different CO_2 concentration, all CO_2 recorders were calibrated, and a regression line for each recorder was determined. The average RMSE between the reference and calibrated value was 3.8 ppm (Max 17.0 ppm), and all measured values were corrected based on the regression line.

2.2. Experimental condition and procedure

To understand the effect of the correlation between supply airflow momentum and buoyancy, as mentioned above, the indoor temperature and contaminant distribution were measured. The experimental conditions are shown in Table 1. The ventilation system (IJV versus DV), the number of supply terminals, and the combination of the supply flow rate and temperature were the experimental parameters. The total heat generation rate was set to be 1,000 W (50 W × 20), which equals to 36.7 W/m^2.

Although the walls, floor and ceiling of the climate chamber was insulated and the climate chamber is located inside of the main laboratory, there might be slight heat transmission through walls. Since the experiment under cooling mode was conducted in winter, the target exhaust temperature was set to be lower than standard condition to make the thermal condition close to adiabatic as much as possible. Therefore, the target exhaust temperature in this experiment was set to be 17 °C, while standard exhaust temperature was assumed to be around 26 °C

Table 1. Experimental conditions.

Case	Number of terminals	Supply condition (total flow rate and temperature)				Supply velocity [m/s]
		250 m³/h (ACH: 3.3) Ts = 5 °C (ΔT = 12 °C)	300 m³/h (ACH: 4.0) Ts = 7 °C (ΔT = 10 °C)	375 m³/h (ACH: 5.0) Ts= 9 °C (ΔT = 8 °C)	500 m³/h (ACH: 6.6) Ts= 11 °C (ΔT = 6 °C)	
IJV-1a	1	X				3.93
IJV-1b			X			4.72
IJV-1c				X		5.89
IJV-1d					X	7.86
IJV-2a	2	X				1.96
IJV-2b			X			2.36
IJV-2c				X		2.95
IJV-2d					X	3.93
DV-1a	1	X				0.37
DV-1b			X			0.44
DV-1c				X		0.55
DV-1d					X	0.74
DV-2a	2	X				0.18
DV-2b			X			0.22
DV-2c				X		0.28
DV-2d					X	0.37

for cooling mode. Given the climate chamber is adiabatic, it is the temperature difference from supply and exhaust temperature that was regarded as the important factor. When the supply temperature and correspondingly room temperature is decreased compared to standard condition, the decreased room air temperature distribution is interpreted to be almost simply shifted by the same extent without changing its distribution feature, and it must be noted that this temperature shift causes no loss in generality when we consider the results of temperature distribution and ventilation effectiveness. The number of terminals was changed to understand the effect of supply momentum on air distribution performance without changing total supply flow rate. Additionally, both total supply flow rate and supply temperature were also changed while keeping the same rate of heat flow under the adiabatic assumption. The studied case of supply temperature (Ts) was 57,911 °C, of which purpose was to change the temperature difference between supply and exhaust air (ΔT) to 12,108 and 6 °C respectively. Correspondingly, supply flow rate was changed from 250 to 500 m³/h to change supply air velocity from 3.93 to 7.68 m/s. Thus, experimental condition was set to change the combination of supply momentum and temperature difference (ΔT).

The time schedule of the experiment is shown in Figure 4. At first, the supply flow rate was verified by continuous dosing of the tracer gas based on stationary concentration method (ISO, 2017). After the indoor temperature reached the steady state, CO_2 gas was emitted continuously at a rate of 60 L/h in total, i.e. 15 L/h at each emission point. After the CO_2 concentration reached the steady state, the state was kept for 1–3 hours. Here, it was interpreted to be the steady state when exhaust temperature doesn't change more than 0.2 °C within an hour, and exhaust CO_2 concentration doesn't change more than 10 ppm within thirty minutes. The results averaged over the last 30 minutes were adopted as the experimental results, though the results were almost stable. The measurement interval of temperature and CO_2 concentration was one minute.

3. Definition of index

Definition of the key indices used in this paper is explained in this section. As for the temperature, three kinds of indices are defined in dimensionless form and evaluated in this paper. The first index is the temperature at the ankle level. Since the cooled air is directly supplied to the occupied zone in DV and IJV system, there are over-cooling risks around ankle level. To evaluate this, the dimensionless temperature around the ankle is defined by:
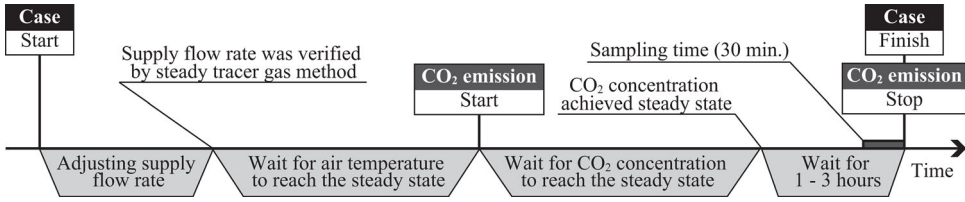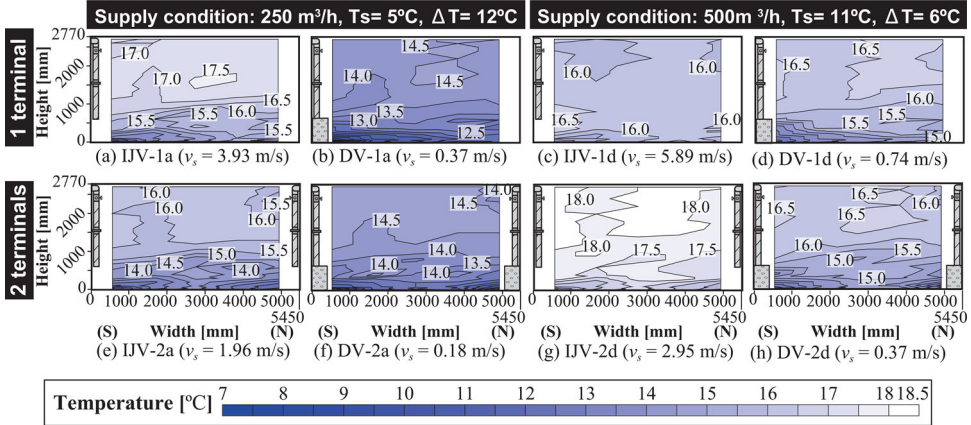
Figure 4. Time schedule of the experiments.

Figure 5. Comparison of temperature contours.

$$T_{Ak}{}^* = \frac{T_{0.1} - T_s}{T_e - T_s},\tag{1}$$

where, $T_{0.1}$ (°C) is the horizontal-average temperature at the height of 0.1 m. $T_{Ak}{}^*$ is naturally equal to one in the mixing condition. The second index is the spatial average temperature within the occupied zone. Since both DV and IJV are a type of stratified ventilation, it is the occupied zone that must be kept comfortable. To evaluate this, in this paper, the following dimensionless temperature is defined:

$$T_{OZ-h_{oz}}{}^* = \frac{\frac{1}{h_{oz}} \int_0^{h_{oz}} T_h dh - T_s}{T_e - T_s},\tag{2}$$

where, T_h is the horizontal-average temperature at a height of h, and h_{oz} (m) is the height of occupied zone. Here, two cases are assumed and evaluated as the height of occupied zone. Namely, $h_{oz} = 1.1$ (m) for seated condition, and $h_{oz} = 1.7$ (m) for standing condition, and dimensionless temperature is expressed as $T_{OZ-1.1}{}^*$ and $T_{OZ-1.7}{}^*$ respectively. These indices also become one in the mixing ventilation. The third index is the vertical temperature difference. While stratified ventilation provides relatively high ventilation effectiveness, there is a possibility of causing an undesirable vertical temperature difference in terms of thermal comfort. Thus, the dimensionless vertical temperature difference between ankle level and head level is defined by:

$$T_{VD-h_{oz}}{}^* = \frac{T_{h_{oz}} - T_{0.1}}{T_e - T_s},\tag{3}$$

Assuming seated and standing condition, as well as Equation (2), both 1.1 m and 1.7 m are adopted, and dimensionless temperature difference is expressed as $T_{VD-1.1}$ or $T_{VD-1.7}$. This index is equal to zero in the mixing condition. It must be noted that in evaluating thermal comfort, not dimensionless temperature but temperature difference itself becomes important. For instance, in

Table 2. Actual experimental conditions.

| Case | Target temperature (°C) | | Measured temperature (°C) | | | Supply flow rate (m³/h) | | Error (%) |
	Temperature difference	Supply	Supply	Exhaust	$T_{2.7}$	Target	Tracer gas measurement	
IJV-1a	5	12	4.7	17.1	17.3	250	235	6.1
IJV-1b	7	10	6.6	15.0	15.2	300	300	0.0
IJV-1c	9	8	9.1	15.3	15.7	375	375	0.1
IJV-1d	11	6	11.2	15.8	16.1	500	484	3.1
IJV-2a	5	12	4.4	16.0	16.2	250	262	−4.8
IJV-2b	7	10	6.2	16.3	16.5	300	295	1.8
IJV-2c	9	8	9.1	17.7	17.9	375	354	5.6
IJV-2d	11	6	10.6	17.7	18.2	500	479	4.3
DV-1a	5	12	4.4	14.4	14.4	250	241	3.7
DV-1b	7	10	6.3	14.6	14.6	300	310	−3.4
DV-1c	9	8	8.7	14.9	15.0	375	376	−0.2
DV-1d	11	6	10.9	16.3	16.5	500	516	−3.3
DV-2a	5	12	4.5	14.5	14.4	250	266	−6.3
DV-2b	7	10	6.6	14.0	14.0	300	315	−5.1
DV-2c	9	8	8.4	14.7	14.6	375	387	−3.3
DV-2d	11	6	10.4	16.3	16.4	500	510	−2.0

ASHRAE standards 55 (ASHRAE, 2013), temperature difference between head level and ankle level shall not exceed 3 °C (5.4 °F). This corresponds to 'Category A' in ISO 7730 (ISO, 2005). In this context, dimensional value seems to be required. However, this paper aims to organise correlation between these indices and Archimedes number calculated from several design conditions, which is explained later. Based on this correlation, dimensional temperature difference can easily be predicted.

As for the contaminant concentration, two indices for ventilation effectiveness are evaluated in this paper. As the first index, the contaminant removal effectiveness (CRE), ε^c, is evaluated that is introduced in the REHVA guidebook (Mundt et al., 2004) by using the following equation:

$$\varepsilon^c = \frac{C_e - C_s}{\frac{1}{H_c} \int^{H_c} C_h dh - C_s},$$
(4)

where, C_e and C_s are the CO_2 concentration of exhaust and supply air, respectively, and C_h is the horizontal-averaged concentration at the height of h. In a fully mixed situation, CRE is equal to 1.0 because the concentration in the exhaust is the same as in the whole room. As the second index regarding ventilation effectiveness, the dimensionless CO_2 concentration within the occupied zone, C_n, is provided in SHASE Standard 102 in Japan (SHASE, 2011), which is defined as:

$$C_n = \frac{\frac{1}{1.8} \int_0^{1.8} C_h dh - C_s}{C_e - C_s}.$$
(5)

High ventilation effectiveness gives a small value of C_n, while it gives a large value of ε^c. The practical role of C_n in ventilation design is that when installing a high-efficiency ventilation system, e.g. DV and IJV systems, the ventilation rate can be decreased to $C_n \times 100\%$ in comparison with the ventilation requirement in MV to achieve the same environment in the occupied zone.

One of the purposes of this paper is to provide a simple method to predict these indices, thus, empirical equations are expected to be obtained. In a room with an IJV system, these indices are expected to be significantly affected by a number of factors, and they seem to vary between MV and DV. As mentioned in the introduction, supply temperature and momentum seem to be the most important factors. Therefore, the Archimedes number is adopted as a parameter to predict above-shown indices because it considers both inertial and buoyancy force. In this paper, the following specific Archimedes number (Ar_{room}) was defined and adopted:

Table 3. Dimensionless temperature results.

Case	Number of terminals	Supply flow rate (m³/h)	$Ar_{room} \times 10^2$ (-)	Dimensionless temperature (-)				
				T_{Ak}^*	$T_{OZ-1.1}^*$	$T_{OZ-1.7}^*$	$T_{VD-1.1}^*$	$T_{VD-1.7}^*$
IJV-1a	1	250	0.41	0.76	0.87	0.91	0.20	0.24
IJV-1b		300	0.20	0.78	0.87	0.91	0.16	0.23
IJV-1c		375	0.10	0.83	0.91	0.94	0.11	0.16
IJV-1d		500	0.04	0.88	0.97	0.97	0.09	0.10
IJV-2a	2	250	1.54	0.74	0.85	0.90	0.23	0.27
IJV-2b		300	0.94	0.73	0.84	0.90	0.24	0.28
IJV-2c		375	0.51	0.73	0.87	0.91	0.22	0.28
IJV-2d		500	0.25	0.77	0.91	0.93	0.16	0.23
DV-1a	1	250	148.7	0.82	0.91	0.93	0.12	0.18
DV-1b		300	86.0	0.88	0.97	0.97	0.10	0.11
DV-1c		375	41.5	0.89	0.99	0.99	0.11	0.09
DV-1d		500	20.8	0.99	1.13	1.12	0.14	0.10
DV-2a	2	250	591.2	0.75	0.85	0.90	0.20	0.25
DV-2b		300	307.1	0.77	0.88	0.92	0.16	0.23
DV-2c		375	163.8	0.78	0.89	0.92	0.15	0.22
DV-2d		500	89.4	0.86	0.99	0.99	0.13	0.11

Notes. When calculating Ar_{room} and T^*, the horizontal-averaged temperature at the height of FL + 2.7 m ($T_{2.7}$) was adopted as T_e.

$$Ar_{room} = \frac{g\beta H_c(T_e - T_s)}{v_s^2}, \qquad (6)$$

where, g is the gravity acceleration (9.8 m/s²), β is the thermal expansion coefficient, H_c is the height of the room (= 2.77 m), T_e is the temperature of exhaust air as the target temperature, T_S is the temperature of supply air, and v_s is the supply velocity. Given T_e can roughly be estimated by assuming certain heat loss condition, Ar_{room} can be obtained by design conditions, such as supply temperature, supply flow rate, target temperature, room shape and inlet shape. Therefore, it is expected that by obtaining the correlation between Ar_{room} and indoor environment indices, it is possible to predict the indoor environment in the design phase. In order to express the inlet condition, Kobayashi also defined Ar_{SA}, which adopted the temperature difference between the supply air and the air at lower level of the room, which is entrained into the jet (Kobayashi et al., 2019). However, since the aim of this paper is to provide the prediction method available in a design phase, the input parameter shall be obtained from the design conditions. The temperature of the entrained air at the lower level cannot be easily estimated from design conditions, but that itself is the target to be predicted. Thus, Ar_{room} which can be obtained by only design parameters is adopted as an explanatory variable to predict indoor environmental indices for IJV system.

4. Results and discussion

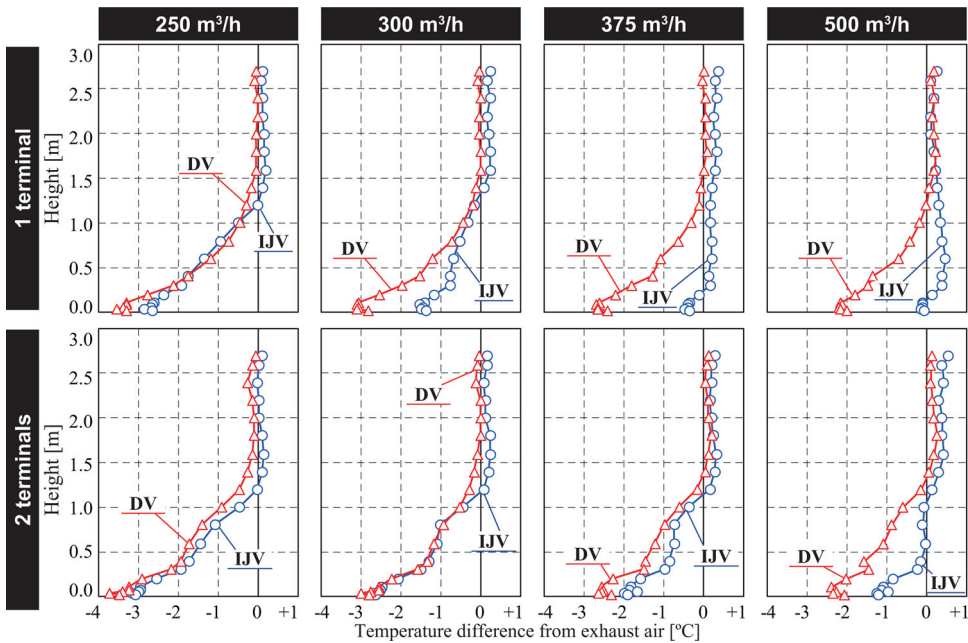### 4.1. Temperature distribution

The actual conditions controlled in the experiments are summarised in Table 2. The value of Ar_{room} and the calculated results of the dimensionless temperatures are shown in Table 3. The results of these indices are discussed later in relation to Archimedes number in Section 4.3.1. When calculating Ar_{room} and the dimensionless temperatures, the horizontal-averaged temperature at the height of FL + 2.7 m ($T_{2.7}$) was adopted as T_e because the exhaust duct was not insulated, and the temperature inside the duct was slightly lower than that of the higher part of the room. Thus, it was interpreted that the temperature measured inside the exhaust duct was affected by the temperature at the attic. Therefore, $T_{2.7}$ was adopted as the temperature of the air actually exhausted from the room.

Temperature distributions of the north-south central cross-section are shown as contours in Figure 5. In the Case IJV series with a small supply flow rate, the vertically stratified temperature distribution is formed, while it cannot be seen with a large supply flow rate. On the other hand, in the Case DV series, the temperature stratified clearly in all cases.

Vertical distributions of horizontal-averaged temperature difference from exhaust air are shown in Figure 6. It is shown that the number of supply terminals has a large influence on the temperature distribution in the cases with IJV. In DV, the temperature profile did not differ depending on the number of terminals. In the cases with IJV, the temperature distribution stratified clearly when the supply flow rate was small, and an almost uniform profile can be seen when the flow rate was large. As the supply flow rate increases, the temperature distribution was similar to that of the mixing condition. On the other hand, the more the supply flow rate decreases, the more similar the temperature distribution to that of DV. In the cases of a small supply flow rate with two terminals, the results of DV and IJV were almost the same despite the difference in supply velocity. This is because the supply momentum in the IJV was small enough to work as low-momentum ventilation like DV due to the small flow rate. As a result, the temperature distribution of IJV is shown to be similar to that of the mixing condition with large supply momentum and to that of DV with small supply momentum. It can be interpreted that the temperature profile in IJV is more sensitive to supply air condition, while it does not significantly differ in DV under the same condition of total rate of input heat flow. This seems to be a difficulty in designing a HVAC system with IJV, and leads to a need for the simplified prediction method. As mentioned in the previous section, therefore, the specific Archimedes number Ar_{room} is used to provide the correlation with the predicted dimensionless temperature, which is to be discussed later in Section 4.3.1.

In general, the temperature ratio around the floor, defined by

$$Temperature\ ratio = \frac{T_h - T_s}{T_e - T_s}, \tag{7}$$

Figure 6. Vertical distribution of normalised horizontal-averaged room temperature comparing by the ventilation system (Blue circles: IJV; Red triangles: DV).
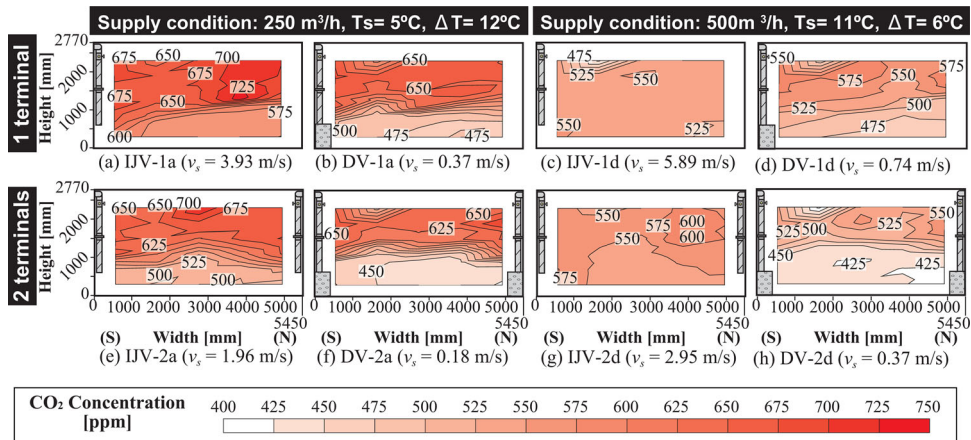
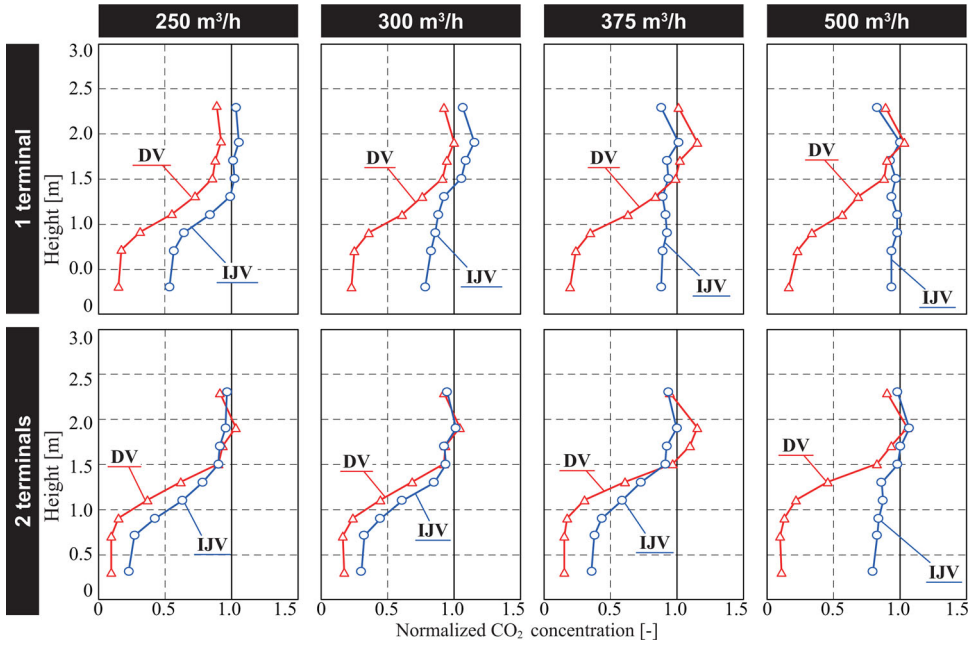**Figure 7.** Comparison of CO_2 concentration contours.

Table 4. Supply/exhaust CO_2 concentration, ε^c and C_n.

Case	Number of terminals	Supply flow rate (m³/h)	CO_2 concentration (ppm) Supply	CO_2 concentration (ppm) Exhaust	ε^c (-)	C_n (-)
IJV-1a	1	250	431	687	1.18	0.74
IJV-1b		300	427	627	1.04	0.89
IJV-1c		375	415	576	1.12	0.90
IJV-1d		500	415	539	1.08	0.95
IJV-2a	2	250	449	678	1.49	0.52
IJV-2b		300	427	630	1.45	0.53
IJV-2c		375	429	598	1.44	0.56
IJV-2d		500	441	566	1.09	0.87
DV-1a	1	250	439	688	1.66	0.44
DV-1b		300	419	612	1.52	0.50
DV-1c		375	448	608	1.42	0.54
DV-1d		500	455	572	1.60	0.46
DV-2a	2	250	420	646	1.73	0.38
DV-2b		300	408	599	1.61	0.43
DV-2c		375	422	577	1.61	0.43
DV-2d		500	417	535	1.83	0.33

is approximately equal to 0.65 in the displacement ventilated room with the distributed heat sources (Kosonen et al., 2002). Here, the temperature ratio around the floor was calculated by using the temperature at a height of 20 mm, $T_{0.02}$, as T_h. The average temperature ratio of IJV was 0.829 (standard deviation: 0.087) and that of DV was 0.660 (standard deviation: 0.014). It was shown that the temperature ratio around the floor was approximately the same as the literature value in the cases of DV, while it becomes larger in IJV cases. This indicates that in IJV the temperature at the lower level can be kept higher in comparison with DV, where over cooling around the floor can be a problem.

4.2. Co2 concentration distribution

The measurement results of the CO_2 concentration of supply air and exhaust air, ε^c, and C_n, are shown in Table 4. The contours of CO_2 concentration on the north-south central cross-section are shown in Figure 7. In Case IJV series, the CO_2, as a contaminant, stratified vertically with small supply flow rate, and relatively uniform distribution was seen with large flow rate. Compared to the thermal stratification, in general, CO_2 forms a clearer stratification because it works as almost passive scalar. In the cases with one supply terminal, non-uniform horizontal

Figure 8. Vertical distribution of horizontal-averaged room normalised CO_2 concentration comparing by the ventilation system (Blue circles: IJV; Red triangles: DV).

distribution can be seen, as well as temperature distribution, when the supply momentum was small. As shown in Case IJV-1a, though fresh air was supplied from the terminal mounted on the south wall, the CO_2 concentration around the lower part of the room was lower than that in the north part of the room. It was assumed that after the impingement on the floor, the jet started spreading with a thin layer. As the jet spreads, the thickness of the jet increases due to the entrainment of the ambient air and the jet rose upward when it reached the heating elements. Thus, the CO_2 concentration was relatively high in the south area, which was close to the supply terminal.

The vertical profiles of the horizontal-averaged normalised CO_2 concentration, $C_h{}^*$, are shown in Figure 8. This normalised concentration is defined as follows:

$$C_h{}^* = \frac{C_h - C_s}{C_e - C_s}.$$

(8)

$C_h{}^*$ approaches one for mixing ventilation. In all cases, as the supply momentum decreases, the CO_2 concentration stratified clearly. The vertical stratification was clearer in the distribution of CO_2 concentration than in that of temperature because the heat could be transferred by radiation while the CO_2 was carried as a passive contaminant by advection and diffusion (Heiselberg & Sandberg, 1990). Thus, the CO_2 concentration reflects the effect of supply airflow conditions on its vertical profile and also shows the fresh air distribution feature more clearly than the temperature. In the Case DV, there exists a difference of CO_2 concentration distribution depending on the number of supply terminals, while no clear difference could be seen in the temperature distribution. DV provides the stratification in the cases with one supply terminal, and the cases with IJV showed uniform distributions, except for the case of the smallest supply flow rate. In the cases with a large supply flow rate, the results of DV and IJV were completely different. IJV can work as MV under the supply condition of high momentum, while it acts like DV when the supply momentum is low. In addition, the supply momentum was found to have a significant influence on contaminant concentration.

In order to make the emitted CO_2 rise up within thermal plume, the emission point of CO_2 was set just above the heating element, which is 600 mm above the floor. However, 600 mm was possibly too low for simulating the contaminant emission from human, and the low emission point could have made the height of contaminant interface (the height that vertical contaminant concentration suddenly changes) lower than actual phenomenon. Therefore, the method for simulating heat and contaminant generation from human remained as issues to be discussed.

4.3. Correlation between the Archimedes number and various indices

4.3.1. Dimensionless temperature

The results of dimensionless temperature T^*, defined in Section 2.3, are summarised in Table 3. The correlation between Ar_{room} and dimensionless temperatures are shown in Figure 9. As Ar_{room} increases, i.e. as supply momentum decreases, T^* approaches constant values in IJV cases. Here, the empirical equation between T^* and Ar_{room} for IJV is expressed by the following equation:

$$T^* = a \times \left\{ 1 - \exp(-b \times Ar_{room}) \right\} + c, \tag{9}$$

where, c is 1.0 for T_{Ak}^*, $T_{OZ-1.1}^*$, and $T_{OZ-1.7}^*$, and 0 for $T_{VD-1.1}^*$ and $T_{VD-1.7}^*$. The empirical equations obtained by the least squares method and the RMSE from the measured results are shown in Table 5. The regression curve for IJV by Equation (9) is indicated in Figure 9, and the averaged value among all DV cases is also added.

As Ar_{room} increases, i.e. as supply momentum decreases, the T^* value of IJV approaches that of DV, and the asymptotic value ($a + c$ in Equation (9)) exists between the values of perfect mixing condition and DV. The dimensionless temperature at ankle height, T_{Ak}^*, was higher in IJV than that of DV, even when Ar_{room} increases. This means that IJV could avoid the over-cooling risk, compared to DV. The dimensionless temperatures within the occupied zone, $T_{OZ-1.1}^*$ and $T_{OZ-1.7}^*$, were lower in DV compared to IJV. However, when Ar_{room} increases, these values are approximately the same for DV and IJV. This means that IJV has almost the same cooling performance within the occupied zone as DV. The dimensionless vertical temperature differences, $T_{VD-1.1}^*$ and $T_{VD-1.7}^*$, were obviously smaller in IJV than in DV. It seems that IJV can avoid the risks of an unpleasant vertical temperature difference between the head and ankle, which can frequently be a problem in operating a stratified ventilation system like DV.

RMSE values of the empirical equations were quite small. This indicates that by using the equations, the indoor thermal environment of a room with IJV can be roughly but easily predicted from Ar_{room}, which can be determined by design factors.

Top: dimensionless temperature at the height of ankle (T_{AK}^*), Middle: dimensionless temperature within occupied zone (T_{OZ}^*), Bottom: dimensionless differential temperature between the height of head and ankle.

4.3.2. Removal of contaminant

The correlation between Ar_{room} and two indices, contaminant removal effectiveness (ε^c) and dimensionless contaminant concentration within the occupied zone (C_n), are shown in Figure 10. It was shown that in IJV, as Ar_{room} increases, both ε^c and C_n approach constant values between those of MV and DV. Similar to the dimensionless temperature discussed in the previous section, the correlation can be expressed by the empirical equation:

$$\varepsilon^c \text{ or } C_n = a \times \left\{ 1 - \exp(-b \times Ar_{room}) \right\} + c, \tag{10}$$

where, $c = 1.0$ in both indices.

The obtained empirical equations and the RMSE from the measured results are summarised in Table 6. The regression curve from Equation (10) is added in Figure 10. In IJV, the larger Ar_{room} is, the better the values of ε^c and C_n. Comparing the asymptotic values of IJV with the averaged
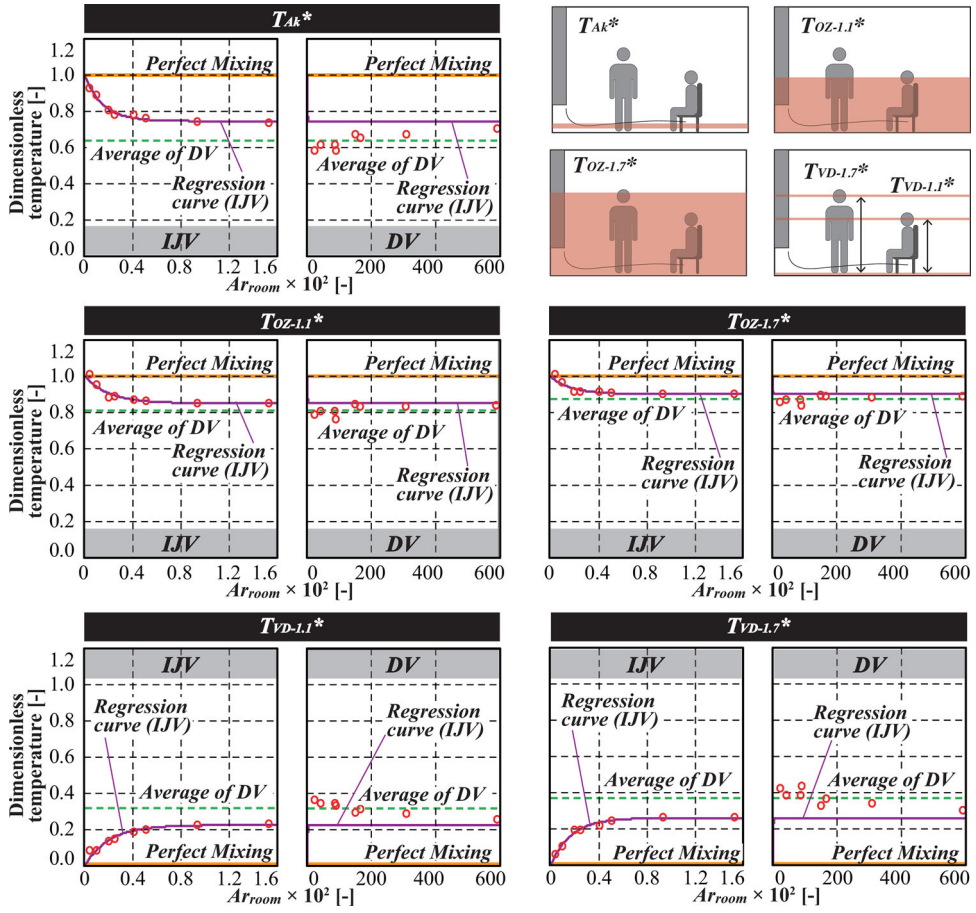
Figure 9. Relationship between Archimedes number and dimensionless temperature.

Table 5. Value of variables and Archimedes number.

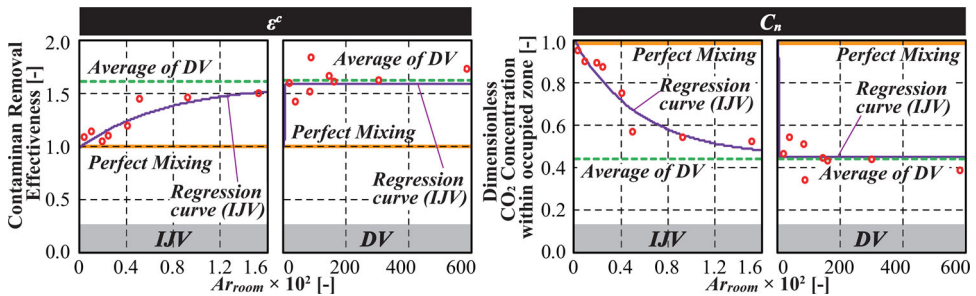| Empirical equation for IJV	RMSE	Asymptotic value ($a + c$)	Averaged value of DV
$T_{Ak}{}^* = -0.25\{1 - \exp(-6.6 \times 10^2 \times Ar_{room})\} + 1.0$	0.029	0.75	0.64
$T_{OZ-1.1}{}^* = -0.15\{1 - \exp(-4.9 \times 10^2 \times Ar_{room})\} + 1.0$	0.048	0.85	0.81
$T_{OZ-1.7}{}^* = -0.10\{1 - \exp(-5.8 \times 10^2 \times Ar_{room})\} + 1.0$	0.037	0.90	0.87
$T_{VD-1.1}{}^* = 0.22\{1 - \exp(-4.9 \times 10^2 \times Ar_{room})\}$	0.050	0.22	0.32
$T_{VD-1.7}{}^* = 0.26\{1 - \exp(-5.7 \times 10^2 \times Ar_{room})\}$	0.027	0.26	0.37

Figure 10. Correlation between Archimedes number and contaminant removal indices. Left: Contaminant removal effectiveness (ε^c), Right: Dimensionless contaminant concentration within occupied zone (C_n).

Table 6. Variable and Archimedes number values.

Equation	RMSE	Asymptotic value $(a + c)$	Averaged value of DV
$\varepsilon^c = 0.59\{1 - \exp(-1.3 \times 10^2 \times Ar_{room})\} + 1.00$	0.22	1.59	1.62
$C_n = -0.55\{1 - \exp(-1.8 \times 10^2 \times Ar_{room})\} + 1.00$	0.15	0.45	0.44

value of DV, one can see that DV exhibits slightly better contaminant removal performance than IJV. The RMSE values of the empirical equation are relatively small as well as the dimensionless temperature. By using these equations, ventilation effectiveness for IJV can be estimated based on design conditions as well as above-shown dimensionless temperatures.

5. Conclusion

To understand the benefits and shortcomings of IJV compared to DV, full-scale experiments were conducted in a climate chamber with heating elements distributed inside. The ventilation system (IJV and DV), and supply air conditions were adjusted in the study. The results were evaluated by analysing the correlation between Archimedes number and indices of cooling and contaminant removal performance. It was shown that DV has slightly better cooling performance and contaminant removal effectiveness as those of IJV, when the specific Archimedes number was large. However, IJV can avoid the overcooling risk and unpleasant vertical temperature difference, which could be a problem in the operation of DV, while keeping high ventilation effectiveness.

The major findings obtained in this study are summarised as follows:

- In IJV, the more the supply momentum decreases, the more temperature and CO_2 concentration were clearly stratified. Thus, IJV can work as MV under the supply condition of high momentum, and can also work as DV with low momentum. It is concluded that by adjusting the design condition of IJV, there is a possibility to be able to control the distribution of indoor temperature and contaminant concentration as designer intends.
- To date, criterion of supply condition for IJV was not well understood, and even the data to be able to design appropriate IJV system was not sufficiently provided. Therefore, empirical equations were finally shown in this paper as a simple prediction method to obtain the requirement for designing IJV. By using these equations, the indoor thermal environment and contaminant removal effectiveness of a room with IJV can be roughly but easily predicted from the Archimedes number, which can be determined by design factors. Simultaneously, when designer have an indoor design target to be accomplished at the room, the Archimedes number, i.e. supply condition, can be determined by the empirical equations.

The current experimental investigation was limited to the indoor environment of a room with IJV and DV under cooling condition. As the heat generation from human and other apparatuses was simulated by heating elements, and were distributed uniformly inside the climate chamber without dynamic load, the experiment was not ideally practical. However, the present experiment is the first step that should be done to understand the feature of IJV. The experimental conditions were set systematically, so the results accumulated by the experiments are believed to provide the quantitative comparison of IJV and DV. Moreover, the correlations between design parameters and indoor environment indices are also believed to contribute to the future works. More results of parametric studies are need to be accumulated.

Disclosure statement

Funding

Notes on contributors

Haruna Yamasawa is a PhD student at the Department of Architectural Engineering, Osaka University in Japan and is a research fellow of Japan Society for the Promotion of Science. Her research includes indoor air quality, thermal comfort, air distribution and thermal energy storage.

Tomohiro Kobayashi is an associate professor at the Department of Architectural Engineering, Osaka University in Japan. His research includes ventilation, air distribution, indoor air quality, thermal comfort, and HVAC-systems in buildings.

Toshio Yamanaka is a professor at the Department of Architectural Engineering, Osaka University in Japan. His research includes ventilation, indoor air quality, thermal comfort, air distribution and odor evaluation.

Narae Choi is a specially appointed assistant professor at the Department of Architectural Engineering, Osaka University in Japan. Her research includes indoor air quality, thermal comfort, air distribution and odor evaluation.

Mako Matsuzaki serves as facility designer at Nikken Sekkei Ltd. in Japan. Her research includes indoor air quality, thermal comfort and air distribution.

ORCID

Haruna Yamasawa http://orcid.org/0000-0002-1262-8781
Toshio Yamanaka http://orcid.org/0000-0002-7660-1609

References

Ameen, A., Cehlin, M., Larsson, U., & Karimipanah, T. (2019). Experimental investigation of the ventilation performance of different air distribution systems in an office environment—cooling mode. *Energies*, *12*(7), 1354–1368. https://doi.org/10.3390/en12071354

ASHRAE. (2013). ASHRAE Standard 55-2013: Thermal Environmental Conditions for Human Occupancy. Retrieved from: https://www.ashrae.org/technical-resources/bookstore/standard-55-thermal-environmental-conditions-for-human-occupancy.

Assoum, H. H., Hamdi, J., El Hassan, M., Abed-Meraim, K., El Kheir, M., Mrach, T., El Asmar, S., & Sakout, A. (2020). Turbulent kinetic energy and self-sustaining tones: Experimental study of a rectangular impinging jet using high speed 3D tomographic particle image velocimetry. *Journal of Mechanical Engineering and Sciences*, *14*(1), 6322–6333. https://doi.org/10.15282/jmes.14.1.2020.10.0495

Awbi, H., & Karimipanah, T. (2002). *A comparison between four different ventilation systems* [Paper presentation]. In Roomvent, Copenhagen, Denmark (pp. 181–184). https://doi.org/10.2307/3405502

Boyle, R. (1899). Natural and artificial methods of ventilation. *Nature*, *61*, 72–83. https://doi.org/10.1038/061006a0

Brohus, H., & Nielsen, P. (1996). Personal exposure in displacement ventilated rooms. *Indoor Air*, *6*(3), 157–167. https://doi.org/10.1111/j.1600-0668.1996.t01-1-00003.x

Cao, G., Ruponen, M., & Kurnitski, J. (2010). Experimental investigation of the velocity distribution of the attached plane jet after impingement with the corner in a high room. *Energy and Buildings*, *42*(6), 935–944. https://doi.org/10.1016/j.enbuild.2010.01.005

Chen, H. J., Moshfegh, B., & Cehlin, M. (2012). Numerical investigation of the flow behavior of an isothermal impinging jet in a room. *Building and Environment*, *49*, 154–166. https://doi.org/10.1016/j.buildenv.2011.09.027

Chen, H. J., Moshfegh, B., & Cehlin, M. (2013). Investigation on the flow and thermal behavior of impinging jet ventilation systems in an office with different heat loads. *Building and Environment*, *59*, 127–144. https://doi.org/10.1016/j.buildenv.2012.08.014

Chen, H., Moshfegh, B., & Mathias, C. (2013). Computational investigation on the factors influencing thermal comfort for impinging jet ventilation. *Building and Environment*, 66, 29–41. https://doi.org/10.1016/j.buildenv.2013.04.018

Fatemi, I., Wang, B. C., Koupriyanov, M., & Tully, B. (2013). Experimental study of a non-isothermal wall jet issued by a displacement ventilation system. *Building and Environment*, 66, 131–140. https://doi.org/10.1016/j.buildenv.2013.04.019

Habchi, C., Ghali, K., & Ghaddar, N. (2015). Displacement ventilation zonal model for particle distribution resulting from high momentum respiratory activities. *Building and Environment*, 90, 1–14. https://doi.org/10.1016/j.buildenv.2015.03.007

Heiselberg, P., & Sandberg, M. (1990). *Convection from a slender cylinder in a ventilated room* [Paper presentation]. In: Roomvent, Norway.

ISO. (2005). ISO-7730: Ergonomics of the Thermal Environment — Analytical Determination and Interpretation of Thermal Comfort Using Calculation of the PMV and PPD Indices and Local Thermal Comfort Criteria. Retrieved from: https://www.iso.org/standard/39155.html International Organization for Standardization.

ISO. (2017). ISO-12569: Thermal Performance of Buildings and Materials - Determination of Specific Airflow Rate in Buildings - Tracer Gas Silution Method Retrieved from: https://www.iso.org/standard/69817.html.

Karimipanah, T., & Awbi, H. B. (2002). Theoretical and experimental investigation of impinging jet ventilation and comparison with wall displacement ventilation. *Building and Environment*, 37(12), 1329–1342. https://doi.org/10.1016/S0360-1323(01)00117-2

Karimipanah, T., Sandberg, M., & Awbi, H. B. (2000). *A comparative study of different air distribution systems in a classroom* [Paper presentation]. In Roomvent, Reading, United Kingdom (pp. 1013–1018).

Kobayashi, T., Nishiumi, T., & Umemiya, N. (2019). *Simplified prediction method of vertical temperature distribution for impinging jet ventilation system* [Paper presentation]. In: CLIMA 2019 Congress, Bucharest, Romania. https://doi.org/10.1051/e3sconf/201,911,101,097

Kobayashi, T., Sugita, K., Umemiya, N., Kishimoto, T., & Sandberg, M. (2017). Numerical investigation and accuracy verification of indoor environment for an impinging jet ventilated room using computational fluid dynamics. *Building and Environment*, 115, 251–268. https://doi.org/10.1016/j.buildenv.2017.01.022

Kosonen, R., Melikov, A., Mundt, E., Mustakallio, P., & Nielsen, P. V. (2002). Displacement Ventilation, Rehva Guidebook No. 23. Brussels: REHVA.

Li, Y., Sandberg, M., & Fuchs, L. (1992). Vertical temperature profiles in rooms ventilated by displacement: Full-scale measurement and nodal modelling. *Indoor Air*, 2(4), 225–243. https://doi.org/10.1111/j.1600-0668.1992.00005.x

Lin, Z., Chow, T. T., & Tsang, C. F. (2007). Effect of door opening on the performance of displacement ventilation in a typical office building. *Building and Environment*, 42(3), 1335–1347. https://doi.org/10.1016/j.buildenv.2005.11.005

Mathisen, H. M. (1989). Case studies of displacement ventilation in public halls. *ASHRAE Transactions*, 95, 1018–1027.

Melikov, A. K., & Nielsen, J. B. (1989). Local thermal discomfort due to draft and vertical temperature difference in rooms with displacement ventilation. *ASHRAE Transactions*, 95, 1050–1057.

Mundt, E. (1995). Displacement ventilation systems - Convection flows and temperature gradients. *Building and Environment*, 30(1), 129–133. https://doi.org/10.1016/0360-1323(94)E0002-9

Mundt, E., Martin, H., Peter, M., Nielsen, V., & Moser, A. (2004). Ventilation Effectiveness, Rehva Guidebook No. 2. Brussels: REHVA The Society of Heating, Air-Conditioning and Sanitary Engineers of Japan..

Nielsen, P. V. (1993). Displacement Ventilation -Theory and Design. Aalborg University.

Nielsen, P. V. (2001). *The "family tree" of air distribution systems* [Paper presentation]. In: Roomvent, Trondheim, Norway, 2011.

Park, H. J., & Holland, D. (2001). The effect of location of a convective heat source on displacement ventilation: CFD study. *Building and Environment*, 36(7), 883–889. https://doi.org/10.1016/S0360-1323(01)00014-2

Rajaratnam, N. (1976). *Turbulent jet*. Elsevier Science Ltd.

Sandberg, M., & Blomqvist, C. (1989). Displacement ventilation systems in office rooms. *ASHRAE Transactions*, 95, 1041–1049.

Seppanen, O. A., Fisk, W. J., Eto, J., & Grimsrud, D. T. (1989). Comparison of conventional mixing and displacement air-conditioning and ventilating systems in U.S. commercial buildings. *ASHRAE Transactions*, 95, 1028–1040.

SHASE. (2011). Ventilation Requirements for Acceptable Air Quality [In Japanese], Retrieved from: http://www.shasej.org/tosho/shase-s.html.

Skistad, H. (1994). Displacement Ventilation. Research Studies Press Ltd. International Organization for Standardization.

Sun, W., Cheong, K. W. D., & Melikov, A. K. (2012). Subjective study of thermal acceptability of novel enhanced displacement ventilation system and implication of occupants' personal control. *Building and Environment*, 57, 49–57. https://doi.org/10.1016/j.buildenv.2012.04.004

Suzuki, T., Sagara, K., Yamanaka, T., Kotani, H., & Yamashita, T. (2007). Vertical profile of contaminant concentration in sickroom with lying person ventilated by displacement. In: *IAQVEC 2007 Proceedings, Sendai, Japan* (pp. 369–376).

Svensson, A. G. L. (1989). Nordic experience of displacement ventilation systems. *ASHRAE Transactions*, *95*, 1013–1017.

Wu, X., Olesen, B. W., Fang, L., & Zhao, J. (2013). A nodal model to predict vertical temperature distribution in a room with floor heating and displacement ventilation. *Building and Environment*, *59*, 626–634. https://doi.org/10.1016/j.buildenv.2012.10.002

Xing, H., Hatton, A., & Awbi, H. B. (2001). A study of the air quality in the breathing zone in a room with displacement ventilation. *Building and Environment*, *36*(7), 809–820. https://doi.org/10.1016/S0360-1323(01)00006-3

Xu, M., Yamanaka, T., & Kotani, H. (2001). Vertical profiles of temperature and contaminant concentration in rooms ventilated by displacement with heat loss through room envelopes. *Indoor Air*, *11*(2), 111–119. https://doi.org/10.1034/j.1600-0668.2001.110205.x

Yamanaka, T., Kotani, H., & Xu, M. (2007). *Zonal models to predict vertical contaminant distribution in room with displacement ventilation accounting for convection flows along walls* [Paper presentation]. IAQVEC 2007 Proceedings - 6th International Conference on Indoor Air Quality, Ventilation and Energy Conservation in Buildings: Sustainanle Built Environment, Sendai, Japan.

Ye, X., Kang, Y., Yan, Z., Chen, B., & Zhong, K. (2020). Optimization study of return vent height for an impinging jet ventilation system with exhaust/return-split configuration by TOPSIS method. *Building and Environment*, *177*, 106858. https://doi.org/10.1016/j.buildenv.2020.106858

Ye, X., Kang, Y., Yang, F., & Zhong, K. (2019). Comparison study of contaminant distribution and indoor air quality in large-height spaces between impinging jet and mixing ventilation systems in heating mode. *Building and Environment*, *160*, 106159. https://doi.org/10.1016/j.buildenv.2019.106159

Ye, X., Kang, Y., Yang, X., & Zhong, K. (2018). Temperature distribution and energy consumption in impinging jet and mixing ventilation heating rooms with intermittent cold outside air invasion. *Energy and Buildings*, *158*, 1510–1522. https://doi.org/10.1016/j.enbuild.2017.11.038

Ye, X., Kang, Y., Zuo, B., & Zhong, K. (2017). Study of factors affecting warm air spreading distance in impinging jet ventilation rooms using multiple regression analysis. *Building and Environment*, *120*, 1–12. https://doi.org/10.1016/j.buildenv.2017.03.044

Ye, X., Zhu, H., Kang, Y., & Zhong, K. (2016). Heating energy consumption of impinging jet ventilation and mixing ventilation in large-height spaces: A comparison study. *Energy and Buildings*, *130*, 697–708. https://doi.org/10.1016/j.enbuild.2016.08.055

Yuan, X., Chen, Q., & Glicksman, L. R. (1998). A critical review of displacement ventilation. *ASHRAE Transactions*, *104* (Part 1A), 78–90.

Yuan, X., Chen, Q., & Glicksman, L. R. (1999). Models for predictions of temperature difference and ventilation effectiveness with displacement ventilation. *ASHRAE Transactions*, *105*, 353–367.

Yuan, X., Chen, Q., Glicksman, L. R., Hu, Y., & Yang, X. (1999). Measurements and computations of room airflow with displacement ventilation. *ASHRAE Transactions*, *105*, 340–352.